

**Distance-redshift relation in an isotropic inhomogeneous universe II:**  
Spherically symmetric dust-shell universe

Norimasa Sugiura\*, Ken-ichi Nakao† and Tomohiro Harada‡  
*Department of Physics, Kyoto University, Sakyo-ku, Kyoto 606-8502, Japan*

The relation between the angular diameter distance and redshift ( $d_A$ - $z$  relation) in a spherically symmetric dust-shell universe is studied. We have discovered that the relation agrees with that of an appropriate Friedmann-Lemaître (FL) model if we set a “homogeneous” expansion law and a “homogeneous” averaged density field. This will support the averaging hypothesis that a universe looks like a FL model in spite of small-scale fluctuations of density field, if its averaged density field is homogeneous on large scales. We also study the connection of the proper mass of a shell with the mass of gravitationally bound objects. Combining this with the results of the  $d_A$ - $z$  relation, we discuss an impact of the local inhomogeneities on determination of the cosmological parameters through the observation of the locally inhomogeneous universe.

**I. INTRODUCTION**

The standard big bang model is based on the assumption of the homogeneous and isotropic distribution of matter and radiation. This assumption then leads to the Robertson-Walker (RW) spacetime geometry and the Friedmann-Lemaître (FL) universe model§ through the Einstein equation. This standard model has succeeded in explaining various important observational facts: Hubble’s expansion law, the content of light elements and the existence of the cosmic microwave background radiation (CMBR) [1].

The CMBR conversely gives a strong observational basis for the assumption of homogeneity and isotropy of our universe by its highly isotropic distribution together with the assumption that we are not in any special position in the universe (the Copernican principle). In fact, the deviation of our universe from a homogeneous and isotropic space is as small as  $\sim 10^{-5}$  at the stage of decoupling [2]. Thus our universe is well approximated by a FL model before this stage. On the other hand, the present universe is highly inhomogeneous on small scales; the density contrast against the cosmic background density is of the order of  $10^{30}$  for the sun,  $10^5$  on galactic scales, and of the order of unity even on the scale of superclusters. We have to go beyond FL models and linear perturbations in considering such systems.

We usually regard that a FL model is a large-scale “average” of a locally inhomogeneous universe (averaging hypothesis). Even though the observational data are consistent with the picture that our universe is described well by a RW metric with small perturbations, we are not sure how to derive the background FL model from the inhomogeneous universe by any averaging procedure, or how the non-linear inhomogeneities on small scales affect large-scale behavior of the universe [3]. Although one can derive a background FL model from observations of the nearby galaxies with any rule of averaging one likes, it is uncertain whether this background FL model (or its time evolution backward) agrees well with the highly homogeneous universe at the early regime. The discrepancies might appear, for example, in the estimate of the density of baryonic matter, the density parameter, the age of our universe, and so on. These still remain a non-trivial question to which we have to give a clear answer.

Before proceeding to discuss these problems, we should make the meaning of the term “average” definite. Averaging can be defined as a mapping between an inhomogeneous spacetime and a homogeneous one. This mapping is not

---

\*Email address: sugiura@tap.scphys.kyoto-u.ac.jp

†Email address: nakao@tap.scphys.kyoto-u.ac.jp

‡Email address: harada@tap.scphys.kyoto-u.ac.jp

§We use the term “Robertson-Walker spacetime” when we focus on geometrical aspects of a homogeneous and isotropic model, and “Friedmann-Lemaître model” when we discuss its dynamics and observable quantities.

restricted to simple volume averaging; other averaging methods such as deformation of three-geometry according to the Ricci-Hamilton flow may be possible [4]. By averaging, anyway, we expect that the large-scale (or coarse grained) behavior of the inhomogeneous spacetime is extracted.

Averaging problem has been often studied from the viewpoint of the so-called back-reaction problem, i.e., how the small-scale inhomogeneities affect the global dynamics when averaged on larger scales. Using the perturbation formalism and volume averaging, the back-reaction problem has been studied by several authors [5–9]. Apart from the problem whether the volume averaging is appropriate or not, one reason which makes the discussion of averaging unclear is that there exists no natural choice of time slice in an inhomogeneous universe. This leads to an ambiguity in the definition of averaged expansion rate or averaged density. Actually, there are even apparent discrepancies in the statements of the papers above.

One possible prescription to avoid this difficulty is to treat observable quantities which we can give a clear definition. From this viewpoint, observational effects on the CMBR of small-scale inhomogeneities have been studied [11,12]. These are significant in the sense that the back reactions on the observable quantities were discussed (see, e.g., [14] for a recent discussion of observable quantities in the Lemaitre-Tolman-Bondi spacetime). However, the problem how to determine the cosmological parameters by observing an inhomogeneous universe seems to have been overlooked.

In Sugiura *et al.*(1998; hereafter Paper I) [10], we investigated the distance-redshift relation in a spherically symmetric dust-shell model, and compared it with that of a FL model. We focused on a highly (locally) inhomogeneous model; we prepared pressureless fluid distributed in discrete shells, which cannot be described by small perturbations of a FL background. We discussed the relation between the behavior of the  $d_A$ - $z$  relation and the conditions on the initial time slice concerning the mass density and the expansion rate. We found that the distance-redshift relation observed at the center obeys a FL-like relation, even when there exist only several shells in the initial horizon scale, if the following conditions are satisfied on the initial spacelike hypersurface: the expansion law is homogeneous and the density which is averaged on larger scales than the inhomogeneity scale is scale-independent (i.e., large-scale homogeneity of density field). Here the averaged density is defined simply by dividing the mass of shells by the volume of the hypersurface.

Our previous analysis was, however, limited to a spatially flat case (the Einstein de-Sitter model). There is a claim that the Einstein-de Sitter solution is in a special position as a solution of the Einstein equation; it is a kind of fixed point under renormalization group flow defined by the scaling properties of the Einstein equation [13]. Thus, there is a possibility that our results were due to the special behavior of the perturbations of the Einstein-de Sitter model under an averaging procedure. In this paper, we treat non-flat cases and show that statements similar to those of our previous paper do hold. We also answer some questions unsolved in Paper I. In particular, the previous study of spatially flat cases could not answer which mass should be used in defining the average density, proper mass which appears in the stress-energy tensor of dust shell, or gravitational mass which specifies the parameter of the Schwarzschild spacetime; they are the same in the spatially flat model. Also it will be shown that the significance of the effect of inhomogeneities has curvature dependence.

We here note three interesting points of the dust-shell model. First, its dynamics is exactly solved; it is not necessary to assume the existence of homogeneous background in order to obtain the evolution of matter distribution. Secondly, it treats a discrete mass distribution where the linear perturbation theory is invalid, and also can treat a highly general-relativistic situation where the scale of inhomogeneities are comparable to the horizon scale. In a sense, spherical dust-shell model is a limit case of the Tolman-Bondi solution. We expect it can represent the Tolman-Bondi and the FL solutions when we take appropriate limits where the number density of dust shell goes to infinity, though no rigorous proof has been yet obtained. Thirdly, the motion of each shell can be extended even after shell-crossing occurs. This theme is discussed elsewhere [15,16].

In order to get an insight into the inhomogeneous universe from the study of the dust-shell universe, we will also investigate the origin of the dust shell. Assuming that the dust shell is composed of highly bound objects, we consider the effect of the binding energy of each object on the dynamics of the universe.

The organization of this paper is as follows. In the next section, we summarize the basic equations for the dynamics of a dust-shell universe, distance to the shells from the center, and redshift of the shells measured by an observer at the center. This is an extension of the treatment in Paper I. We give our results and discussion on  $d_A$ - $z$  relation and averaged density in Sec. III. In this section, we also discuss the universe filled with gravitationally bound objects and the effect of the binding energy of each object on the dynamics of the universe. Finally Sec. IV is devoted to the summary.

We follow the sign convention of the Riemann tensor and the metric tensor in [17] and adopt the unit of  $G = c = 1$ .

## II. FORMULATION OF DUST-SHELL UNIVERSE

## A. Equation of motion of dust shell

First, we derive the expansion law of the dust-shell universe. We consider a number of spherically symmetric shells with a common center at  $r = 0$  (see Fig. 1). We label each shell by  $1, 2, \dots, i, \dots$  from inside. The region enclosed by the first shell is the Minkowski spacetime and is labeled as the first region. Similarly, the region enclosed by the  $(i - 1)$ th shell and  $i$ th shell, which is a vacuum, is labeled as the  $i$ th region. Each shell is infinitesimally thin, characterized by the surface stress-energy tensor  $S^{ab}$  which is given by

$$S^{ab} \equiv \lim_{\epsilon \rightarrow 0} \int_{-\epsilon}^{+\epsilon} T^{ab} dx, \quad (2.1)$$

where  $x$  is a Gaussian coordinate ( $x = 0$  on the shell) in the direction normal to the trajectory of the shell.

Since each region between the shells is a vacuum, the spacetime is described by the Schwarzschild geometry by Birkhoff's theorem. The line element in the  $i$ th region is written in the form

$$ds_i^2 = - \left( 1 - \frac{2m_{gi}}{r} \right) dt^2 + \left( 1 - \frac{2m_{gi}}{r} \right)^{-1} dr^2 + r^2 d\Omega^2, \quad (2.2)$$

where the parameter  $m_{gi}$  will be referred to as a gravitational mass ( $m_{g1} = 0$ ), and  $d\Omega^2$  is the line element of a unit sphere.

We derive the expansion law of a dust shell following [18–21]. Let  $n^a$  be a unit spacelike vector normal to the trajectory of the shell, and define the projection operator  $h_a^b \equiv \delta_a^b - n_a n^b$ . From the projected Einstein equation

$$R_{ab} h_c^a h_d^b = 8\pi \left( T_{ab} - \frac{1}{2} g_{ab} T \right) h_c^a h_d^b, \quad (2.3)$$

one obtains

$$\mathcal{L}_n K_{cd} + {}^3 R_{cd} - K K_{cd} = 8\pi \left( T_{ab} h_c^a h_d^b - \frac{1}{2} h_{cd} T \right), \quad (2.4)$$

where  $\mathcal{L}_n$  is the Lie derivative along  $n^a$  and  ${}^3 R_{cd}$  is the three-dimensional Ricci tensor of the timelike hypersurface generated by the motion of the shell. The extrinsic curvature  $K_{ab}$  is defined by  $K_{ab} = -\frac{1}{2} h_a^c h_b^d \mathcal{L}_n h_{cd}$ , and  $K = K_a^a$ ,  $T = T_a^a$ . Integration of Eq. (2.4) over an infinitesimal range along  $n^a$  yields

$$K_{ab}^+ - K_{ab}^- = 8\pi \left( S_{ab} - \frac{1}{2} h_{ab} S \right), \quad (2.5)$$

where the suffix '+' denotes a quantity evaluated at the outside of the shell, and '-' at the inside. Using Eq. (2.5) and the Gauss-Codazzi relation  $2G_{ab} n^a n^b = -{}^3 R + K_{ab} K^{ab} - K^2$ , one finds that the following relation holds for a dust shell:

$$S^{ab} (K_{ab}^+ + K_{ab}^-) = 0. \quad (2.6)$$

The stress-energy tensor of a dust shell is given by

$$S^{ab} = s u^a u^b, \quad (2.7)$$

where  $u^a$  is the 4-velocity of the observer rest on the shell, and  $s$  is the surface energy density of the shell. Combining Eqs. (2.5), (2.6) and (2.7), we obtain the following equation for the circumferential radius  $r_i$  of the  $i$ th shell (the "expansion law" of the dust shell):

$$\left( \frac{dr_i}{d\tau} \right)^2 = \frac{2\bar{M}_i}{r_i} + \left\{ \left( \frac{M_-(i)}{m_s(i)} \right)^2 - 1 \right\} + \frac{m_s^2(i)}{4r_i^2}, \quad (2.8)$$

where  $\bar{M}_i$  and  $M_-(i)$  are defined by

$$\bar{M}_i \equiv \frac{m_{gi} + m_{gi+1}}{2}, \quad (2.9)$$

$$M_-(i) \equiv m_{g^{i+1}} - m_{g^i}, \quad (2.10)$$

and  $\tau$  is the proper time which is measured by an observer rest on the shell. The ‘‘proper mass’’  $m_s(i)$  of the shell is defined by

$$m_s(i) = 4\pi s_i r_i^2 \quad (2.11)$$

where  $s_i \equiv -S_a^a(i)$ . It can be shown this proper mass is a constant of motion by the conservation law,  $S_{a;b}^b = 0$ , where the semicolon denotes the three-dimensional covariant derivative on the trajectory of the shell. We shall assume the energy condition  $m_s \geq 0$ .

In this paper, we use a common proper time  $\tau$  for all the shells. The relation between  $\tau$  and the time coordinate,  $t$ , in the Schwarzschild spacetime is obtained as follows. First, note that two Schwarzschild time coordinates are assigned to each shell: the  $i$ th shell has the time  $t_{(-)i}$  measured in the  $i$ th region and  $t_{(+)i}$  measured in the  $(i+1)$ th region. From Eqs.(2.5) and (2.6), we obtain

$$\frac{dt_{(+)i}}{d\tau} = \left( \frac{r_i}{r_i - 2m_{g^{i+1}}} \right) \left[ \frac{M_-(i)}{m_s(i)} - \frac{m_s(i)}{2r_i} \right], \quad (2.12)$$

$$\frac{dt_{(-)i}}{d\tau} = \left( \frac{r_i}{r_i - 2m_{g^i}} \right) \left[ \frac{M_-(i)}{m_s(i)} + \frac{m_s(i)}{2r_i} \right]. \quad (2.13)$$

The procedure to determine the origin of each time coordinate will be described later.

## B. Cosmological parameters and initial condition

In order to specify a dust-shell universe, we have to fix the parameters in Eq. (2.8) and the initial hypersurface. We first rewrite Eq. (2.8) in the form corresponding to the Hubble equation of a FL model. We denote the initial circumferential radius of the  $i$ th shell by  $x_i$ , i.e.,

$$r_i = x_i \quad (2.14)$$

on initial hypersurface. We define  $\rho_i$  by

$$\bar{M}_i \equiv \frac{4}{3}\pi\rho_i x_i^3, \quad (2.15)$$

and  $k_i$  by

$$\frac{M_-(i)}{m_s(i)} \equiv E_i \equiv \sqrt{1 - k_i x_i}. \quad (2.16)$$

Here  $E_i$  is the specific energy of the  $i$ th shell.  $E_i$  is positive through the space in the open and flat FL models and inside the maximum radius in the closed model. In this paper, we consider the cases where  $E_i > 0$ .

Using these parameters, the expansion law of the dust shell can be written as

$$\left( \frac{1}{r_i} \frac{dr_i}{d\tau} \right)^2 = \frac{8}{3}\pi\rho_i \left( \frac{x_i}{r_i} \right)^3 - k_i \left( \frac{x_i}{r_i} \right)^2 + \frac{m_s^2(i)}{4r_i^4}. \quad (2.17)$$

We see that the first term behaves like a non-relativistic matter term in the Hubble equation of a FL model, the second and the third like a curvature and a radiation source term. From this point of view,  $\rho_i$  and  $k_i$  play roles of the ‘‘energy density’’ and the ‘‘curvature’’, respectively. The radiation-like term might be regarded as the effect of the binding energy of the shell [20]. Further it is worthwhile to note that this radiation-like term is consistent with the result of Futamase [5] about the effect of the small-scale inhomogeneities on the global cosmic expansion. Seeing this, one may expect that the inhomogeneities tend to make the Hubble parameter larger compared with a homogeneous universe which has the same ‘‘energy density’’ of non-relativistic matter. However, this radiation-like term does not necessarily imply the larger Hubble parameter. In order to see the effect of this term on the Hubble parameter, we need to investigate the distance-redshift relation by solving the null geodesic equations and compare the result in the inhomogeneous spacetime and that of the FL model. We will discuss this point later.

A dust-shell universe is specified if we set the parameters contained in Eq. (2.17), i.e.,  $\rho_i$ ,  $k_i$ ,  $x_i$ , and an initial hypersurface. When we increase the number of the shells to infinity with  $\rho_i$  and  $k_i$  being finite and independent

of  $i$  (we will mention this limit as “large  $N$  limit”), the dust-shell universe approaches a FL universe if we take an appropriate initial hypersurface, as we will see in Sec. III. Then the parameters  $\rho_i$  and  $k_i$  agree with the ordinary energy density and curvature in the Hubble equation.

We need to derive the expression of  $t_{(\pm)i}$  in terms of  $r_i$  for the later use. The relations between  $t_{(\pm)i}$  and  $r_i$  are given by [we denote  $m_s(i)$  as  $m_i$  in the remainder of this section]

$$\frac{dt_{(\pm)i}}{dr_i} = \frac{\xi_i(E_i r_i^2 \mp \frac{1}{2} m_i r_i)}{(r_i - 2\bar{M}_i \mp E_i m_i) \sqrt{X_i(r_i)}}, \quad (2.18)$$

where

$$X_i(r_i) = (E_i^2 - 1)r_i^2 + 2\bar{M}_i r_i + \frac{m_i^2}{4}, \quad (2.19)$$

and  $\xi_i$  is the sign of  $dr_i/d\tau$ . This is integrated to give

$$t_i|_{\pm} = \xi_i T_{i\pm}(r_i) + \xi_i (2\bar{M}_i \pm E_i m_i) \ln \left| \frac{2\bar{M}_i}{G_{i\pm}(r_i)} (r_i - 2\bar{M}_i \mp E_i m_i) \right| + \mathcal{T}_{i\pm}, \quad (2.20)$$

where  $\mathcal{T}_{i\pm}$  are integration constants. The functions  $T_{i\pm}(r)$  and  $G_{i\pm}(r)$  are given for  $E_i^2 = 1$  as

$$T_{i\pm}(r) = \frac{1}{3\bar{M}_i^2} \left( \bar{M}_i r + 6\bar{M}_i^2 \pm \frac{3}{2} \bar{M}_i m_i - \frac{m_i^2}{4} \right) \sqrt{X_i(r)}, \quad (2.21)$$

$$G_{i\pm}(r) = \left\{ \sqrt{X_i(r)} + 2\bar{M}_i \pm \frac{m_i}{2} \right\}^2, \quad (2.22)$$

for  $E^2 > 1$  as

$$T_{i\pm}(r) = \frac{E_i}{E_i^2 - 1} \sqrt{X_i(r)} + \left\{ \frac{E_i(2E_i^2 - 3)\bar{M}_i \pm (2E_i^2 - 1)(E_i^2 - 1)\frac{m_i}{2}}{(E_i^2 - 1)\sqrt{E_i^2 - 1}} + 2\bar{M}_i \pm E_i m_i \right\} \\ \times \ln \left[ \bar{M}_i + (E_i^2 - 1)r + \sqrt{E_i^2 - 1} \sqrt{X_i(r)} \right], \quad (2.23)$$

$$G_{i\pm}(r) = \left\{ \sqrt{E_i^2 - 1} r + \sqrt{X_i(r)} + 2 \left( E_i - \sqrt{E_i^2 - 1} \right) \bar{M}_i \pm \frac{1}{2} \left( E_i - \sqrt{E_i^2 - 1} \right)^2 m_i \right\}^2, \quad (2.24)$$

and for  $E^2 < 1$  as

$$T_{i\pm}(r) = \frac{E_i}{E_i^2 - 1} \sqrt{X_i(r)} + \left\{ \frac{E_i(2E_i^2 - 3)\bar{M}_i \pm (2E_i^2 - 1)(E_i^2 - 1)\frac{m_i}{2}}{(E_i^2 - 1)\sqrt{1 - E_i^2}} \right\} 2\text{ArcTan} \left( \sqrt{\frac{r+k}{h-r}} \right), \quad (2.25)$$

$$G_{i\pm}(r) = \left\{ \sqrt{(h - 2\bar{M}_i \mp E_i m_i)(k+r)} + \sqrt{(k + 2\bar{M}_i \pm E_i m_i)(h-r)} \right\}^2, \quad (2.26)$$

where  $h$  and  $-k$  are the roots of  $X_i(r) = 0$ ;

$$h = \frac{\bar{M}_i + \sqrt{\bar{M}_i^2 + (1 - E_i^2)m_i^2/4}}{(1 - E_i^2)}, \quad (2.27)$$

$$k = -\frac{\bar{M}_i - \sqrt{\bar{M}_i^2 + (1 - E_i^2)m_i^2/4}}{(1 - E_i^2)}. \quad (2.28)$$

There is a coordinate singularity on the Killing horizon in the Schwarzschild coordinate;  $t_{(\pm)i}$  becomes infinite on  $r_i = 2m_{gi}$ . In order to avoid this coordinate singularity, and for further calculation, the Kruskal null coordinate is convenient since we will treat the null geodesics in this spacetime. Outside the horizon in the  $i$ th region,  $r > 2m_{gi}$ , the Kruskal null coordinates are given by

$$U \equiv -4\sqrt{m_{gi}(r - 2m_{gi})} \exp \left( \frac{r-t}{4m_{gi}} \right), \quad (2.29)$$

$$V \equiv +4\sqrt{m_{gi}(r - 2m_{gi})} \exp \left( \frac{r+t}{4m_{gi}} \right), \quad (2.30)$$

where  $U$  and  $V$  correspond to the retarded time and the advanced time, respectively. Using these Kruskal coordinates, the line element in the  $i$ th region is expressed as

$$ds_i^2 = -\frac{m_{gi}}{r} \exp\left(-\frac{r}{2m_{gi}}\right) dU dV + r^2 d\Omega^2. \quad (2.31)$$

Similarly to the Schwarzschild time coordinate, two pairs of Kruskal null coordinates,  $U_{(\pm)i}$  and  $V_{(\pm)i}$ , are assigned to each shell. Using Eq. (2.20), we obtain the Kruskal null coordinates labeling the  $i$ th shell in the form

$$U_{(\pm)i}(r_i) = -4\sqrt{\bar{M}_i \pm \frac{E_i}{2}m_i(2\bar{M}_i)^{-\xi_i/2}(r_i - 2\bar{M}_i \mp E_i m_i)^{\frac{1}{2}(1-\xi_i)} G_{i\pm}^{\frac{1}{2}\xi_i}(r_i)} \exp\left[\frac{r_i - T_{i\pm}(r_i) - \mathcal{T}_{i\pm}}{4\bar{M}_i \pm 2E_i m_i}\right], \quad (2.32)$$

$$V_{(\pm)i}(r_i) = +4\sqrt{\bar{M}_i \pm \frac{E_i}{2}m_i(2\bar{M}_i)^{\xi_i/2}(r_i - 2\bar{M}_i \mp E_i m_i)^{\frac{1}{2}(1+\xi_i)} G_{i\pm}^{-\frac{1}{2}\xi_i}(r_i)} \exp\left[\frac{r_i + T_{i\pm}(r_i) + \mathcal{T}_{i\pm}}{4\bar{M}_i \pm 2E_i m_i}\right]. \quad (2.33)$$

These coordinates,  $U_{(\pm)i}$  and  $V_{(\pm)i}$ , are finite on  $r_i = 2m_{gi}$  and are well defined also for  $r_i < 2m_{gi}$ . Hence, we will use the expressions (2.32) and (2.33) for any  $r_i$ . For  $\xi_i = +1$ , both  $U_{(\pm)i}$  and  $V_{(\pm)i}$  are negative when  $2m_{gi}$  is larger than  $r_i$ . In this case, the  $i$ th shell with  $r_i < 2m_{gi}$  is located in the white hole part of the Schwarzschild spacetime. On the contrary, for  $\xi_i = -1$ , the  $i$ th shell with  $r_i < 2m_{gi}$  is located in the black hole part.

The determination of the integration constants  $\mathcal{T}_{i\pm}$  corresponds to the choice of the initial hypersurface. The procedure to construct the initial hypersurface we adopt is summarized as follows. First, we choose a unit spacelike vector  $\ell^a$  which is directed outward (i.e., pointing the direction in which label  $i$  increases). Taking this vector as a starting tangential vector, we extend a spacelike geodesic curve until it reaches the second shell. This spacelike geodesic curve defines the simultaneous hypersurface in the region between the first shell and the second shell. Next we extend from this intersection towards the third shell another spacelike geodesic which starts with another spacelike vector at the second shell. This second spacelike geodesic generates a spacelike hypersurface in this region. Repeating this process, we complete the whole initial hypersurface.

From the above procedure, the integration constant of Eq. (2.20) is determined as follows. In the  $i$ th region, the unit tangent vector,  $\ell^a$ , of the spacelike geodesic is written as

$$\ell^t = e_i \left(1 - \frac{2m_{gi}}{r}\right)^{-1}, \quad \ell^r = \sqrt{1 + e_i^2 - \frac{2m_{gi}}{r}}, \quad (2.34)$$

and the other components vanish, where  $e_i$  is an integration constant associated with the geodesic equation. Now a choice of initial time slice reduces to a choice of  $e_i$ . In Sec. III, we will see the connection between the choice of  $e_i$  and the  $d_A$ - $z$  relation. Once we fix  $e_i$ , the equation for the trajectory of the spacelike geodesic in the  $(t, r)$  plane is given by

$$\frac{dt}{dr} = \frac{e_i r^{\frac{3}{2}}}{(r - 2m_{gi})\sqrt{(1 + e_i^2)r - 2m_{gi}}}. \quad (2.35)$$

Integrating the above equation, we obtain

$$t = F_i(r) + D_i, \quad (2.36)$$

where

$$F_i(r) = \frac{e_i \sqrt{r} \sqrt{(1 + e_i^2)r - 2m_{gi}}}{1 + e_i^2} + 2m_{gi} \ln \left( \frac{\sqrt{(1 + e_i^2)r - 2m_{gi}} - e_i \sqrt{r}}{\sqrt{(1 + e_i^2)r - 2m_{gi}} + e_i \sqrt{r}} \right) + \frac{2m_{gi} e_i (3 + 2e_i^2) \ln(\sqrt{(1 + e_i^2)r - 2m_{gi}} + \sqrt{(1 + e_i^2)r})}{(1 + e_i^2)^{3/2}}, \quad (2.37)$$

and  $D_i$  is an integration constant. Initially, we set  $t_{(+i)} = t_{(-i)}$  and  $t_{(\pm)1} = 0$ . Using these relations, we obtain the integration constants,  $\mathcal{T}_{(\pm)i}$ , as

$$\mathcal{T}_{(\pm)i} = \sum_{j=2}^i [F_j(x_j) - F_j(x_{j-1})] - \xi_i \mathcal{T}_{i\pm}(x_i) - \xi_i (2\bar{M}_i \pm E_i m_i) \ln \left| \frac{\bar{M}_i}{G_{i\pm}(x_i)} (x_i - 2\bar{M}_i \mp E_i m_i) \right|. \quad (2.38)$$

### C. Redshift and diameter distance

We consider a light ray which is emitted from each shell toward an observer rest at the center. The light ray travels along a future directed ingoing radial null geodesic, where ‘‘ingoing’’ refers to the direction from a shell toward shells labeled by a smaller number.

An ingoing radial null geodesic is specified by a constant coordinate value  $V$ . We denote the circumferential radius of the  $i$ th shell when it intersects the null geodesic as  $R_i$ . Labeling the outermost shell by  $M$ , the radius  $R_M$  is equal to  $x_M$  (the initial radius of the  $M$ th shell) and hence in the  $M$ th region,  $V = V_{(-)M}(x_M)$  is satisfied along the null geodesic. Thus, on the  $(M - 1)$ th shell, the following relation holds:

$$V_{(+)M-1}(R_{M-1}) = V_{(-)M}(x_M). \quad (2.39)$$

This equation determines  $R_{M-1}$ . By the same procedure, we obtain the circumferential radii of all the shells at the intersection with the null geodesic:

$$V_{(+)i}(R_i) = V_{(-)i+1}(R_{i+1}). \quad (2.40)$$

We can determine  $R_i$  from the given  $R_{i+1}$  through this equation.

In order to derive the expression of redshift, we first write down the components of the null geodesic tangent in the  $i$ th region,  $k^\mu(i)$ , which is given in the Kruskal null coordinate as

$$k^U(i) = \frac{r}{m_{gi}} \exp\left(\frac{r}{2m_{gi}}\right) \omega_i, \quad (2.41)$$

and the other components vanish, where  $\omega_i$  is an integration constant associated with the geodesic equation. We require that the observed frequency of the photon at each shell is uniquely determined. The observed frequency,  $\omega_{\text{ob}}(i)$ , at the  $i$ th shell is given by

$$\omega_{\text{ob}}(i) = -k_\mu(i)u_{(+)}^\mu(i) = \frac{1}{2}\omega_i \frac{dV_{(+)i}}{d\tau}, \quad (2.42)$$

$$\omega_{\text{ob}}(i+1) = -k_\mu(i)u_{(-)}^\mu(i+1) = \frac{1}{2}\omega_i \frac{dV_{(-)i+1}}{d\tau}. \quad (2.43)$$

Eqs. (2.42) and (2.43) gives the relation between  $\omega_{\text{ob}}(i)$  and  $\omega_{\text{ob}}(i-1)$ , for  $i \geq 2$ , as

$$\omega_{\text{ob}}(i) = f(i)\omega_{\text{ob}}(i-1), \quad (2.44)$$

where

$$f(i) \equiv \frac{dV_{(-)i}/d\tau}{dV_{(+)i-1}/d\tau}. \quad (2.45)$$

For the first region, a direct calculation leads to

$$\omega_{\text{ob}}(1) = \left(\frac{dt_{(-)1}}{d\tau} + \frac{dr_1}{d\tau}\right) \omega_{\text{ob}}(0) \equiv f(1)\omega_{\text{ob}}(0), \quad (2.46)$$

where  $\omega_{\text{ob}}(0)$  is the frequency of the light ray observed by an observer rest at the origin  $r = 0$ . Thus, using the above relations, we obtain the redshift of the light ray emitted from the  $i$ th shell toward the observer rest at  $r = 0$  in the form

$$1 + z(i) \equiv \frac{\omega_{\text{ob}}(i)}{\omega_{\text{ob}}(0)} = \prod_{j=1}^i f(j). \quad (2.47)$$

Our next task is to find the angular diameter-distance  $d_A$ . The definition of  $d_A$  is

$$d_A \equiv \frac{D}{\theta}, \quad (2.48)$$

where  $D$  is the physical length of the source perpendicular to the line of sight, and  $\theta$  is the observed angular size. Since the space we are considering is spherically symmetric, the diameter distance from the observer at the center to the  $i$ th shell agrees with the circumferential radius  $R_i$  when the null geodesic intersects it;

$$d_A(i) = R_i. \quad (2.49)$$

Now we can calculate  $d_A$ - $z$  relation in the dust-shell universe using the relations (2.40), (2.47) and (2.49).

### III. RESULTS AND DISCUSSION

#### A. Setting the parameters of dust-shell model

As mentioned in Sec. III the choice of the parameters and the initial hypersurface determines the behavior of a dust-shell universe. Since we are interested in cases which have a FL limit, we set the parameters so that they approach a FL model in the large  $N$  limit.

We set the mass distribution of the shells as

$$\rho_i = \rho_c \text{ (independent of } i), \quad (3.1)$$

and  $k_i$  in Eq. (2.17) as

$$k_i = k_c. \quad (3.2)$$

Using  $\rho_c$  and  $k_c$ , we define parameters  $H_{\text{shell}}$  and  $r_H$  by

$$H_{\text{shell}}^2 \equiv r_H^{-2} \equiv \frac{8\pi}{3}\rho_c - k_c. \quad (3.3)$$

Further, we define

$$\Omega \equiv \frac{8\pi}{3}\rho_c/H_{\text{shell}}^2. \quad (3.4)$$

Then,

$$k_c = (\Omega - 1)H_{\text{shell}}^2. \quad (3.5)$$

In terms of FL models,  $H_{\text{shell}}$ ,  $r_H$  and  $\Omega$  may be regarded as the ‘‘Hubble constant’’, ‘‘Hubble horizon radius’’, and the ‘‘density parameter.’’

For  $x_i$ , we put

$$x_i(\tau_{\text{init}}) = i\Delta x, \quad (3.6)$$

with a constant interval  $\Delta x$

$$\Delta x \equiv \frac{r_H}{N_H}, \quad (3.7)$$

where  $N_H$  is some positive integer.

Before we proceed, we estimate the magnitude of the radiation-like term in Eq. (2.17). From Eqs. (2.9) and (2.15) with  $m_{g1} = 0$ , we find

$$m_{g2n-1} = \frac{1}{N_H^3}(n-1)^2(4n-1)\Omega r_H, \quad (3.8)$$

$$m_{g2n} = \frac{1}{N_H^3}n^2(4n-3)\Omega r_H, \quad (3.9)$$

where  $n$  is a positive integer. From Eqs. (2.10) and (2.16), we find  $m_s(i) = (m_{gi+1} - m_{gi})/E_i$  and thus obtain

$$m_s(2n-1) = \frac{6n^2 - 6n + 1}{N_H^3} \frac{\Omega}{\sqrt{1 - k_i x_i^2}} r_H, \quad (3.10)$$

$$m_s(2n) = \frac{6n^2}{N_H^3} \frac{\Omega}{\sqrt{1 - k_i x_i^2}} r_H. \quad (3.11)$$

Thus, when we consider a large  $N$  limit with fixing  $x_i = r_H(i/N_H)$ , the proper mass  $Gm_s(i) = \mathcal{O}(N_H^{-1})$  is regarded as a small quantity, compared with  $M_+(i)$  and  $m_{gi}$ . That is, the radiation-like term of Eq. (2.17) is of order  $N_H^{-2}$  of the other terms, and can be neglected when  $N_H$  is sufficiently large. We note that when  $k_c$  is positive (i.e.,  $\Omega > 1$ ), the factor  $\Omega/\sqrt{1 - k_i x_i^2}$  in Eqs.(3.10) and (3.11) is larger than unity, and vice versa when  $k_c$  is negative. This means that, in the dust-shell universe, the effect of the local inhomogeneities (caused by condensing masses to a shell) on the expansion rate appears larger in a closed model and smaller in an open model than that in a flat model which has the same  $H_{\text{shell}}$  and  $x_i$ 's.



## B. Distance-redshift relation and averaged density

As described in Sec.II, the choice of  $e_i$  corresponds to choosing an initial hypersurface. We fix the expansion law to be homogeneous, try some choices of  $e_i$ , and study which  $e_i$  makes the distance-redshift relation behave like that of a FL model. We will consider which physical meaning is carried by that choice, especially in terms of averaged density. We have already analyzed spatially flat cases (i.e.,  $k_c = 0$ ) in Paper I, and found that the distance-redshift relation agrees with that of a (spatially flat) FL model quite well when we choose  $e_i$  so that the averaged density is homogeneous. The averaged density inside the  $i$ th shell  $\bar{\rho}(i)$  is defined by dividing the ‘‘mass’’ contained within  $r_i$  by the three-volume  $\text{Vol}(i)$  on the hypersurface up to  $r_i$ . We may call the density field homogeneous when  $\bar{\rho}(i)$  is independent of  $i$ .

We here write down explicitly the three-volume

$$\begin{aligned} \text{Vol}(i) &= 4\pi \int_{r_{i-1}}^{r_i} \frac{r^{\frac{5}{2}}}{\sqrt{(1+e_i^2)r - 2m_{\text{gi}}}} dr \\ &= 4\pi \left[ \sqrt{(1+e_i^2)r - 2m_{\text{gi}}} \left( \frac{r^{5/2}}{3(1+e_i^2)} + \frac{5r^{3/2}m_{\text{gi}}}{6(1+e_i^2)^2} + \frac{5r^{1/2}m_{\text{gi}}^2}{2(1+e_i^2)^3} \right) \right]_{r_{i-1}}^{r_i} \end{aligned} \quad (3.12)$$

$$+ \frac{20\pi m_{\text{gi}}^3}{(1+e_i^2)^{7/2}} \ln \left( \frac{\sqrt{(1+e_i^2)r_i - 2m_{\text{gi}}} + \sqrt{(1+e_i^2)r_i}}{\sqrt{(1+e_i^2)r_{i-1} - 2m_{\text{gi}}} + \sqrt{(1+e_i^2)r_{i-1}}} \right). \quad (3.13)$$

For  $i = 1$ ,  $\text{Vol}(1)$  is equal to  $4\pi r_1^3/3$ .

Let us study homogeneous density cases, as in Paper I. Now we have two kinds of mass in defining the averaged density; proper mass  $m_s(i)$  defined in Eq. (2.11) and gravitational mass  $m_{\text{gi}}$  which determines the dynamics of its outer shells.

We first take the hypersurface so that  $\bar{\rho}(i)$  using the gravitational mass is homogeneous. We can define the gravitational mass of the  $j$ th shell to be the difference between the gravitational mass parameters of the neighboring regions:  $m_{\text{gi}j+1} - m_{\text{gi}j}$  [=  $E_j m_s(j)$ ]. We add the gravitational mass of each shell up to  $i - 1$ , and add only half of the mass of the  $i$ th shell. The averaged density thus defined is given as

$$\bar{\rho}(i) \equiv \left\{ \frac{1}{2} E_i m_s(i) + \sum_{j \leq i-1} E_j m_s(j) \right\} / \sum_{j \leq i} \text{Vol}(j) = \frac{1}{2} (m_{\text{gi}} + m_{\text{gi}i+1}) / \sum_{j \leq i} \text{Vol}(j). \quad (3.14)$$

As one can see from the definition of  $\rho_c$ , the choice of  $\text{Vol}(i)$  (and hence the choice of  $e_i$ ) which makes this averaged density homogeneous, i.e., independent of  $i$  (and equal to  $\rho_c$ ) is

$$\text{Vol}(i) = \frac{4\pi}{3} (r_i^3 - r_{i-1}^3). \quad (3.15)$$

We plot the  $d_A$ - $z$  relation of the dust-shell models fixed in this way in Figs. 2-4 (choice A). The employed parameters are  $\Omega = 1.0, 0.9$  and  $1.1$ ,  $H_{\text{shell}} = 1.0$ , and the number of shells within the initial Hubble radius  $N_{\text{H}}$  is set to be 4 and 10. The outermost shell  $M$  from which a light is emitted is chosen to be  $2.5 \times N_{\text{H}}$ . We also plot the  $d_A$ - $z$  relation in FL models, which is determined by the initial Hubble parameter  $H_{\text{I}}$ , initial density parameter  $\Omega_{\text{I}}$ , and the redshift of the initial time slice  $z_{\text{I}}$ . These parameters are set using the parameters of the corresponding shell model as  $H_{\text{I}} = H_{\text{shell}}$ ,  $\Omega_{\text{I}} = \Omega$ , and  $z_{\text{I}}$  equal to the redshift of the outermost shell for  $N_{\text{H}} = 10$ . In the flat case, the data of the dust-shell models agree with the FL relation as seen in Paper I. In the non-flat cases, however, the FL models chosen in this way do not approximate the dust-shell models. Even when we increase the number density of the shell, no improvement is obtained. Thus, using the gravitational mass of the shell in averaged density is inappropriate.

Next, we try the choice using the proper mass in defining the averaged density,

$$\bar{\rho}(i) \equiv \left\{ \frac{1}{2} m_s(i) + \sum_{j \leq i-1} m_s(j) \right\} / \sum_{j \leq i} \text{Vol}(j). \quad (3.16)$$

After some manipulation, one finds that the volume element should satisfy the relation

$$\text{Vol}(i) = \frac{4\pi}{3} \left( \frac{r_i^3}{E_i} - \frac{r_{i-1}^3}{E_{i-1}} \right) + \left( \frac{1}{E_{i-1}} - \frac{1}{E_i} \right) m_{\text{gi}}, \quad (3.17)$$

in order to make the averaged density  $\bar{\rho}(i)$  equal to  $\rho_c$  (choice B). In a flat model, this choice is the same as choice A. The  $d_A$ - $z$  relations for open and closed models are plotted in Figs. 5 and 6. These plots show that the relations agree quite well with FL models. Thus, we should use the proper mass in defining the averaged density. We note that owing to the amplification of inhomogeneity which appeared in Eqs.(3.10) and (3.11), closed universe shows slight deviation one can notice when compared with the other cases.

For comparison, we try the orthogonal slice, since, in a FL model, the simultaneous hypersurface is orthogonal to the trajectory of matter (choice C). We choose  $e_i$  so that the vector  $\ell^a$  is orthogonal to the trajectory of each shell. From the condition  $\ell_a u_{(+)}^a(i-1) = 0$  at  $r = r_{i-1}$ , we obtain  $e_i = dr_{i-1}/d\tau$ . Fig. 7 shows the  $d_A$ - $z$  relation in this choice\*\*. We can see a mild deviation from the FL model.

### C. Discussion on the dust-shell model

In paper I we concluded that the  $d_A$ - $z$  relation in a dust-shell universe behaves like a flat FL universe, when the following conditions are satisfied: the expansion law resembles the flat FL model; the behavior of averaged density field is scale-independent when we increase the scale of averaging; the averaged density agrees with  $\rho_c$  (defined by Eq.[3.1]). The discreteness nature of the shell model plays no significant role in our spherical model.

However, our analysis was limited to spatially-flat cases (Einstein de-Sitter model). In this paper, we have examined the non-flat cases, and confirmed that the above statement remains valid. Moreover, paper I could not answer which mass should be used in defining the average density, proper mass which appears in the energy-momentum of dust shell, or gravitational mass which specifies the parameter in Schwarzschild spacetime; the latter includes the gravitational potential energy and the kinetic energy of the shell. In the spatially flat models, they balance and the two masses agree with each other. From the results of this paper, now it becomes clear that the proper mass should be used in defining the averaged density. This might at first sound strange since the geometry of each region is determined by the gravitational mass which includes the kinetic energy and the potential energy. Where has their information gone? Reexamining the Hubble equation of FL models and the expansion law of the dust-shell models, one notices that it is contained in the curvature term. In Eq. (2.16), the curvature term is expressed as the ratio of the proper mass to the difference of gravitational mass between the inside and the outside regions. Thus, the curvature gives the ratio of the total energy to the proper mass.

In our model, the expansion law for the circumferential radius is homogeneous when there are enough number of shells; the effect on the expansion rate of density inhomogeneities is small (of order  $N_H^{-2}$ ). Fixing the expansion law like FL, we studied the connection between the  $d_A$ - $z$  relation and the averaged density. We have found that if we make the averaged density (which is defined using the three-volume element of the hypersurface and the proper mass) homogeneous, the  $d_A$ - $z$  relation agrees well with that of a FL model. That is, there exists a strong connection among the homogeneous averaged density, the homogeneous expansion law, and the FL like distance-redshift relation, in spite of the discrete nature (local inhomogeneity of matter distribution) of the dust-shell model. This will support the ‘‘averaging hypothesis’’ that a universe behaves like a FL model in spite of small-scale fluctuations of density field, if its averaged density field is homogeneous on large scales. This implies that even if there exist large wall-like structures, our universe is approximated by a FL model on larger scales if the walls satisfy the above conditions.

Now we give some comments on the small  $N$  cases; the cases where the radiation-like term in the expansion law is not negligible. One may expect that a FL model including radiation term can fit them, but this does not work. It should be noticed that the radiation-like term is inhomogeneous (i.e., dependent on  $i$ ) in the cases considered in this paper. Then, there is no reason one may expect that the behavior of observables obeys a FL like relation; it is natural that we cannot fit them with FL models including radiation term. That is, it is impossible to approximate such an inhomogeneous model that has a significant large-scale inhomogeneity by a FL model.

### D. Implication on the universe filled with bound objects

We can obtain further insight into the treatment of inhomogeneous universes by investigating the dust-shell universe from a different viewpoint, especially in connection with gravitationally bound objects. We discuss its implications on the estimation of the cosmological parameters of a locally inhomogeneous universe.

---

\*\* We only displayed an open model. There is no solution when  $\Omega > 1$  which satisfies the conditions (3.6) and  $\ell_a u_{(+)}^a(i-1) = 0$  simultaneously for  $N_H = 10, M = 25$ .

We start by considering the construction of a dust shell from small particles. In Appendix, we consider momentarily static initial data in which the intrinsic metric of the spacelike hypersurface is conformally flat and there are arbitrary number of compact objects. By construction of the solution, locations of the objects are arbitrary. Hence, by arranging an infinite number of infinitesimal objects with an appropriate procedure, we can construct an infinitesimally thin shell which is momentarily static. As discussed in Appendix, a spherical shell constructed by this procedure is likely to be regarded as a dust shell treated in this paper. Hence, by arranging sufficient number of such shells by the manner shown in this paper, we can obtain a system of compact objects which well imitates a FL universe.

Next, let us consider a closed FL universe filled with baryonic dust fluid and a dust-shell universe (or a universe filled with compact objects) which have the same baryonic mass. The analysis of the dust-shell universe implies that the sum of the proper mass of all the shells in the closed dust-shell universe is the same as the baryonic mass of the closed FL universe, when the distance-redshift relations of these universes well agree with each other. On the other hand, by the investigation in Appendix, we find that the proper mass of a shell is the sum of the gravitational mass of the objects composing the shell. Here we should recall that the gravitational mass of an object is in general different from its baryonic mass; there is a gravitational mass defect and the difference between the gravitational mass and baryonic mass is recognized to be the binding energy of the object. Thus, if the shells are composed of highly bound objects, the sum of the gravitational mass of all the objects is much smaller than the baryonic mass. Therefore, even if the total baryonic mass of the universe composed of gravitationally bound objects is the same as that of the FL universe filled with the baryonic dust fluid, the distance-redshift relations of these universes can highly disagree with each other.

Now let us study the difference between these universes with the same amount of baryonic mass quantitatively. The line element of the closed FL universe filled with the dust fluid is written as

$$ds^2 = -d\tau^2 + a^2(\tau) (d\chi^2 + \sin^2 \chi d\Omega^2). \quad (3.18)$$

The solution of the Einstein equation can be written in the form

$$a = \frac{2M}{3\pi} (1 - \cos \eta), \quad (3.19)$$

$$\tau = \frac{2M}{3\pi} (\eta - \sin \eta), \quad (3.20)$$

where  $M$  is the total mass of the dust and  $0 \leq \eta \leq 2\pi$ . In the dust-shell model, the mass  $M$  is given by the sum of the gravitational mass of all the objects in the universe if the shells are composed of bound objects; we denote it by  $M_G$ . On the other hand, in the FL universe filled with the baryonic dust fluid,  $M$  is the total baryonic mass  $M_B$ . When the two universes have the same amount of baryons,  $M_G < M_B$  holds.

Here we study how the Hubble parameter  $H$  and density parameter  $\Omega$  at a fixed age  $\tau = \tau_0$  change when we change the mass parameter  $M$ . The Hubble parameter and the density parameter are defined by

$$H \equiv \frac{1}{a} \frac{da}{d\tau} = \frac{3\pi \sin \eta}{2M(1 - \cos \eta)^2}, \quad (3.21)$$

$$\Omega \equiv \frac{4M}{3\pi a^3 H^2} = \frac{2(1 - \cos \eta)}{\sin^2 \eta}, \quad (3.22)$$

where  $M$  and  $\eta$  is connected through the relation  $\tau_0 = \frac{2M}{3\pi} (\eta - \sin \eta)$ . Then the derivative of  $M$  with respect to  $\eta$  is given by

$$\left. \frac{\partial M}{\partial \eta} \right|_{\tau_0} = -\frac{3\pi\tau_0(1 - \cos \eta)}{2(\eta - \sin \eta)^2}. \quad (3.23)$$

From Eqs.(3.21), (3.22) and (3.23), we obtain

$$\left. \frac{\partial H}{\partial M} \right|_{\tau_0} = \frac{3\pi \{3(\eta - \sin \eta) - \eta(1 - \cos \eta)\}}{2M^2(1 - \cos \eta)^3}, \quad (3.24)$$

$$\left. \frac{\partial \Omega}{\partial M} \right|_{\tau_0} = -\frac{2(1 - \cos \eta)(\eta - \sin \eta)}{M \sin^3 \eta}. \quad (3.25)$$

One can confirm the positivity of  $\partial H/\partial M$  and hence the Hubble parameter increases with increasing mass  $M$ . On the other hand, the density parameter  $\Omega$  is a decreasing function of  $M$  in the expanding phase while an increasing function

in the contracting phase. This implies that if the dust shells are made of bound objects, the Hubble parameter of the dust-shell universe is smaller, and the density parameter is larger, than those of the FL universe filled with baryonic dust fluid (in the expanding phase) with the same amount of baryons and the same age, since the relation  $M_G < M_B$  holds.

In the limit of  $\tau/M \rightarrow 0$  (accordingly  $\eta \rightarrow 0$ ), the closed FL universe filled with dust fluid behaves like the Einstein-de Sitter universe. The behavior of  $H^{-1}\partial H/\partial M$  in this limit is easily obtained:

$$\left. \frac{1}{H} \frac{\partial H}{\partial M} \right|_{\tau_0} \rightarrow \frac{1}{30M} \quad \text{for} \quad \frac{\tau_0}{M} \rightarrow 0. \quad (3.26)$$

Using the above equation, the difference in the Hubble parameter of the dust-shell universe,  $H_{\text{DS}}$ , and that of the FL universe filled with the baryonic dust fluid,  $H_{\text{FL}}$ , is given by

$$\frac{H_{\text{FL}} - H_{\text{DS}}}{H_{\text{FL}}} \sim \frac{1}{30M_B} (M_B - M_G) < \frac{1}{30}. \quad (3.27)$$

Thus, at the nearly Einstein-de Sitter stage, the effect of the mass defect of the objects in the universe is rather small. (The difference in the density parameters of these universes vanishes in this limit.) On the other hand, at the stage of the maximum expansion  $\eta = \pi$ , the derivatives,  $H^{-1}\partial H/\partial M$  and  $\partial\Omega/\partial M$ , blow up. This is simply because  $H$  goes to 0 at  $\eta = \pi$  and thus the diverging behavior itself has no serious consequence. However, this indicates the tendency that the effect of the binding energy of the compact objects becomes somewhat larger than the Einstein-de Sitter epoch when the curvature of the universe is comparable to the energy density of the dust fluid.

The observation of CMBR strongly suggests that our universe was highly isotropic and homogeneous at least on the last scattering surface. Hence in the study of the universe in the early stages, the linear perturbation analysis is powerful. In order to perform the linear analysis, we need to fix the background FL universe, whose cosmological parameters are usually determined by the observation of our neighborhood. The universe observed today is, however, highly inhomogeneous and the inhomogeneities may prevent the correct determination of the background FL universe. The above discussion implies that taking account of the binding energy may be important in estimating the density parameter and the Hubble parameter near the maximum expansion, if the universe is filled with highly bound objects. On the other hand, when the universe is in the stage when the curvature of the universe is not dominant, the effect of the mass defect is rather small. We note that, however, in order to discuss the physical quantities of the inhomogeneous universe (e.g., the age of the universe) and its whole time evolution using a FL model constructed by the nearby observations, we have to know the behavior of the scale factor in the transition regime from the almost FL universe to the inhomogeneous one. This problem is now under investigation and will be given elsewhere [23].

#### IV. SUMMARY

We studied the behavior of  $d_A$ - $z$  relation in a spherically symmetric dust-shell universe where the mass distribution is discrete. Extending the treatment in our previous paper which only spatially flat models were considered, we analyzed non-flat cases. We compared the distance-redshift relation of dust-shell universe with that of FL models. In particular, we examined the behavior of the averaged density of the dust-shell universe when the two  $d_A$ - $z$  relations are similar. We found that the  $d_A$ - $z$  relation observed at the center agrees quite well with that of a flat FL model if the following conditions are satisfied: (i) the expansion law of the circumferential radius of the shells resembles the Hubble equation of a spatially flat FL model, (ii) the behavior of averaged density around the observer at the center is scale-independent as we increase the scale on which we take the average, and (iii) the averaged density agrees with the energy density of the FL model. In defining the averaged density, we take the total proper mass of the shells and divide it by the three-volume of the initial hypersurface. We noted that the choice of the initial hypersurface relates the expansion law to the averaged density.

The effect of discreteness of mass distribution appears in the equation of motion of each dust shell. This effect becomes smaller as we increase the number density of shell, though we found that the positive curvature has tendency to enhance the inhomogeneity effect. We conclude that, in this spherical dust-shell model, the discrete nature of matter distribution plays no significant role in discussing the observed quantities such as  $d_A$  and  $z$ , as long as the expansion law and the averaged density field is sufficiently homogeneous in the sense described above. This supports the averaging hypothesis that a universe is described by a FL model if the universe is homogeneous when the density is averaged on a large scale than the scale of the inhomogeneities. This may also imply that even if there exist large wall-like structures, our universe is approximated by a FL model on larger scales if the walls satisfy the above conditions.

However, we have to keep in mind that our model is highly idealized and our analysis is limited only to spherically symmetric cases. In general, local inhomogeneities strongly affect the light propagation, giving rise to dispersions in the observed  $d_A$ - $z$  relation [24–26]. It will be also interesting to study cases when the light ray enters a shell in a non-radial direction.

It still remains unclear whether three-dimensional discreteness have a significant effect on the dynamics of the universe. The study of the momentarily static initial data in Appendix strongly suggests that when the universe is filled with bound objects, the dynamics of the universe is determined by the gravitational mass density of the objects but not by the baryonic mass density. The gravitational mass of a compact object is in general different from its baryonic mass due to the gravitational mass defect. The effect of the mass defect on the dynamics of the universe is significant at the stage of the curvature-dominant phase while it is not significant at the early stage of the universe, i.e., the stage during which the universe behaves as the Einstein-de Sitter universe. However, in general, there are both the bound and unbound objects. Hence we should consider a situation including both objects and investigate their effects on the dynamics, which is left for our future work.

## ACKNOWLEDGEMENTS

We would like to thank H. Sato for encouragement. N.S. and T.H. are supported by Japan Society for the Promotion of Science for Young Scientists Grant Nos. 3167 and 9204. This work is partially supported by Grant-in-Aid for Creative Basic Research(09NP0801) and for Scientific Research B(09440106) from the Japanese Ministry of Education, Science, Sports and Culture.

## APPENDIX: MOMENTARILY STATIC INITIAL DATA OF A SPHERICAL SHELL COMPOSED OF BOUND OBJECTS

In order to get an insight into the origin of the proper mass  $m_s$  of a spherical shell, we consider momentarily static initial data of which the extrinsic curvature vanishes. The intrinsic metric of the three-dimensional spacelike hypersurface is assumed to be conformally flat,

$$dl^2 = \psi^4(\vec{x})d\vec{x}^2, \quad (\text{A1})$$

where  $\vec{x}$  is a position vector. Then the Hamiltonian constraint is written as

$$\Delta\psi = -2\pi\rho_H\psi^5, \quad (\text{A2})$$

where  $\Delta$  is the Laplacian operator in the flat space and  $\rho_H$  is the energy density for an observer whose trajectory is normal to the spacelike hypersurface.

We introduce the gravitational mass density defined by

$$\rho_G \equiv \rho_H\psi^5. \quad (\text{A3})$$

Let us consider a situation where  $n$  “spherical” objects exist. We give  $\rho_G$  by

$$\rho_G = \sum_{I=1}^n \rho_{GI}, \quad (\text{A4})$$

where

$$\rho_{GI} = \rho_{GI} (|\vec{x} - \vec{x}_I|) \geq 0, \quad (\text{A5})$$

for  $|\vec{x} - \vec{x}_I| \leq \ell_I$  (radius of the  $I$ th object), while  $\rho_{GI}$  vanishes for  $|\vec{x} - \vec{x}_I| > \ell_I$ . The solution of the Hamiltonian constraint is then written in the form

$$\psi = 1 + \sum_{I=1}^n \psi_I, \quad (\text{A6})$$

where  $\psi_I$  satisfies the equation

$$\Delta\psi_I = -2\pi\rho_{GI}, \quad (\text{A7})$$

with the boundary condition,  $\psi_I \rightarrow 0$  for  $|\vec{x} - \vec{x}_I| \rightarrow \infty$ .

Integrating Eq. (A7), the solution of the Hamiltonian constraint is easily obtained:

$$\psi = 1 + 2\pi \sum_{I=1}^n \int_{|\vec{x}-\vec{x}_I|}^{\infty} dy y^{-2} \int_0^y dx x^2 \rho_{GI}(x). \quad (\text{A8})$$

For the vacuum region, the above solution takes a simple form

$$\psi = 1 + \frac{1}{2} \sum_{I=1}^n \frac{m_I}{|\vec{x} - \vec{x}_I|}, \quad (\text{A9})$$

where the parameter  $m_I$  is defined by

$$m_I \equiv 4\pi \int_0^{\ell_I} dx x^2 \rho_{GI}(x). \quad (\text{A10})$$

We also consider the proper mass  $m_{pI}$  of the  $I$ th object defined by

$$m_{pI} \equiv \int d^3x \rho_{HI} \psi^6 = \int d^3x \rho_{GI} \psi. \quad (\text{A11})$$

If the compact objects are composed of dust fluid,  $m_{pI}$  is the conserved rest mass (baryonic mass). The above integral is easily performed to give

$$m_{pI} = m_I \left( 1 + \delta_I + \frac{1}{2} \sum_{J \neq I} \frac{m_J}{|\vec{x}_I - \vec{x}_J|} \right), \quad (\text{A12})$$

where

$$\delta_I \equiv \frac{1}{m_I} \int d^3x \rho_{GI} \psi_I = \frac{8\pi^2}{m_I} \int_0^{\ell_I} dz z^2 \rho_{GI}(z) \int_z^{\infty} dy y^{-2} \int_0^y dx x^2 \rho_{GI}(x). \quad (\text{A13})$$

Now let us consider the ‘‘gravitational mass’’ of the  $I$ th object, which includes the gravitational binding energy. In order to obtain it, we replace the compact object by an Einstein-Rosen bridge with the same mass parameter  $m_I$ . This means that we employ solution (A9) even inside the object. Now instead of the compact object, we have a ‘‘sheet’’ with an asymptotic region  $|\vec{x} - \vec{x}_I| \rightarrow 0$ . In this asymptotic region, one can define the ADM mass (gravitational mass)  $M_I$  which corresponds to the total energy of the  $I$ th object. Brill and Lindquist [22] showed that  $M_I$  is given by

$$M_I = m_I \left( 1 + \frac{1}{2} \sum_{J \neq I} \frac{m_J}{|\vec{x}_I - \vec{x}_J|} \right). \quad (\text{A14})$$

Then the gravitational binding energy  $E_{\text{bind}}^I$  of the  $I$ th object is naturally defined as

$$E_{\text{bind}}^I = M_I - m_{pI} = -m_I \delta_I. \quad (\text{A15})$$

The above equation implies that  $\delta_I$  is the specific binding energy of the  $I$ th object.

Here let us consider a situation in which compact objects with almost identical mass  $m_I \sim m$  are distributed homogeneously on spheres with a common center labeled by  $i = 1, \dots, N$ . The  $i$ th sphere contains the objects labeled by  $I$  in the range  $n_i + 1 \leq I \leq n_{i+1}$ , where  $n_1 = 0$ ,  $n_i < n_{i+1}$ , and  $n_{N+1}$  is equal to the total number of the objects  $n$ . Note that the position vector of the  $I$ th object on the  $i$ th sphere satisfies  $|\vec{x}_I| = R_i$ . Let us denote the sum of the parameter  $m_I$  inside the  $i$ th region as

$$M_{\text{gi}} \equiv \sum_{I=1}^{n_i} m_I. \quad (\text{A16})$$

We consider a limit where the number of the objects on each shell goes to infinity with  $M_{gi}$  fixed:  $n_{i+1} - n_i \rightarrow \infty$  for all  $i$ 's. By this procedure, we obtain a system of infinitely thin  $N$  spherical shells with a common center. This system has the same configuration as that treated in this paper (see Fig.1). In the limit where  $n_{i+1} - n_i$  is very large, the mean separation,  $L$ , between the objects is given by

$$L \sim \sqrt{\frac{4\pi r_i^2}{n_{i+1} - n_i}}, \quad (\text{A17})$$

while the mass parameter  $m_I$  is

$$m_I \sim \frac{M_{gi+1} - M_{gi}}{n_{i+1} - n_i}. \quad (\text{A18})$$

We assume that the radius of each object is  $\ell_I = \alpha m_I$ , where  $\alpha$  is a constant. If we consider an Einstein-Rosen bridge instead of the object, we choose the constant  $\alpha$  to be  $1/2$ . This assumption implies that in the large- $(n_{i+1} - n_i)$  limit,  $\ell_I/L$  approaches to zero since it is proportional to  $(n_{i+1} - n_i)^{-1/2}$ . Hence a shell obtained by this limit is extremely sparse. In order to know whether the shell obtained by this limiting procedure is a dust shell, we need to study the time evolution of this initial data. Although we do not investigate its time evolution here, it seems likely that a shell composed of infinite number of infinitesimally small objects is a dust shell by the following reason. Since the mean separation between the objects is infinitely larger than the radius of each object, a direct collision between the objects is impossible when the shell is shrinking. Further, since  $m_I/L$  is extremely smaller than unity, the effect of the gravity of a nearby particle which causes a non-radial motion is likely to be very small. These two should work to keep the spherical symmetry and the radial motion of the shell during its evolution.

In order to obtain the relation between  $M_{gi}$  and the mass parameter  $m_{gi}$  of the Schwarzschild spacetime in the  $i$ th region, we investigate the line element in the  $i$ th region. The conformal factor in Eq. (A1) in the  $i$ th region is written as

$$\psi = A_i + \frac{M_{gi}}{2R}, \quad (\text{A19})$$

where  $A_i$  is a constant and  $R \equiv |\vec{x}|$ . From the continuity of the conformal factor, we obtain a recurrent relation for  $A_i$  as

$$A_i = A_{i+1} + \frac{1}{2R_i} (M_{gi+1} - M_{gi}). \quad (\text{A20})$$

Since the value of  $A_{N+1}$  in the outermost region is unity, we can obtain  $A_i$  for  $1 \leq i \leq N$  by the above equation. Eq. (A19) gives the line element as

$$dl^2 = A_i^4 \left( 1 + \frac{M_{gi}}{2A_i R} \right)^4 (dR^2 + R^2 d\Omega^2). \quad (\text{A21})$$

Introducing a new radial coordinate  $X = A_i^2 R$ , the above line element becomes

$$dl^2 = \left( 1 + \frac{A_i M_{gi}}{2X} \right)^4 (dX^2 + X^2 d\Omega^2), \quad (\text{A22})$$

which is the line element of the Schwarzschild spacetime in the isotropic coordinate. Then the mass parameter  $m_{gi}$  is now trivially obtained as

$$m_{gi} = A_i M_{gi}. \quad (\text{A23})$$

As reviewed in Sec. II, the dynamics of an infinitely thin shell is treated by Israel's formalism. The equation for the circumferential radius  $r_i$  of the  $i$ th shell is given by Eq. (2.8):

$$\left( \frac{dr_i}{d\tau} \right)^2 = \left( \frac{M_-(i)}{m_s(i)} \right)^2 - 1 + \frac{2\bar{M}_i}{r_i} + \frac{m_s^2(i)}{4r_i^2}. \quad (\text{A24})$$

The proper mass  $m_s(i)$  of a dust shell is conserved during its time evolution. We will write down  $m_s(i)$  using the mass parameters of the objects composing the shell, by comparing the above equation with the solution of (A1). The

momentarily static situation corresponds to the moment of maximum expansion  $dr_i/d\tau = 0$ . Hence from Eq. (A24), we obtain the relation

$$\left(\frac{M_-(i)}{m_s(i)}\right)^2 - 1 + \frac{2\bar{M}_i}{r_i} + \frac{m_s^2(i)}{4r_i^2} = 0. \quad (\text{A25})$$

In the present situation, we know the gravitational mass  $m_{g_i}$  and the circumferential radius  $r_i$  which is related with  $R_i$  by

$$r_i = R_i \left( A_{i+1} + \frac{M_{g_{i+1}}}{2R_i} \right)^2. \quad (\text{A26})$$

Hence Eq. (A25) is regarded as an algebraic equation to determine the proper mass  $m_s(i)$  of the  $i$ th shell. The positive roots of this equation are given as

$$m_s(i) = m_{s\pm} = r_i \left( \sqrt{1 - \frac{2m_{g_i}}{r_i}} \pm \sqrt{1 - \frac{2m_{g_{i+1}}}{r_i}} \right), \quad (\text{A27})$$

where  $m_{g_i} < m_{g_{i+1}}$  is assumed. In order to make the meanings of the above roots clear, we consider Eq. (2.12). At the moment of the maximum expansion,  $r_i$  should be larger than or equal to  $2m_{g_{i+1}}$ . First we consider the case when  $r_i > 2m_{g_{i+1}}$ . Then we easily find that  $dt_{(+i)}/d\tau$  is negative for  $m_s(i) = m_{s+}$  and positive for  $m_s(i) = m_{s-}$ . Together with Eq. (A26), the positivity of  $dt_{(+i)}/d\tau$  implies that  $m_s(i)$  should be equal to  $m_{s-}$  for  $R_i > m_{g_{i+1}}/2$  (i.e., the direction of the time coordinate  $t_{(+)}$  should agree with that of the proper time  $\tau$  in this asymptotic region), while it should be equal to  $m_{s+}$  for  $R_i < m_{g_{i+1}}/2$ . When  $r_i = 2m_{g_{i+1}}$ , i.e.,  $R_i = m_{g_{i+1}}/2$ , the solution  $m_{s+}$  agrees with  $m_{s-}$  and hence  $m_s(i)$  is equal to  $m_{s\pm}$  in this case.

From Eqs.(A20) and (A23), we find

$$m_{g_i} = \left\{ A_{i+1} + \frac{1}{2R_i} (M_{g_{i+1}} - M_{g_i}) \right\} M_{g_i}, \quad (\text{A28})$$

$$m_{g_{i+1}} = A_{i+1} M_{g_{i+1}}. \quad (\text{A29})$$

Using Eqs.(A26), (A27) and the above equations, we obtain

$$m_s(i) = (M_{g_{i+1}} - M_{g_i}) \left( A_{i+1} + \frac{M_{g_{i+1}}}{2R_i} \right), \quad (\text{A30})$$

imposing  $dt_{(+i)}/d\tau > 0$ . On the other hand, in the spherical-shell limit, the gravitational mass  $M_I$  in Eq. (A14) of the  $I$ th object on the  $i$ th shell becomes

$$M_I \longrightarrow m_I \left( A_{i+1} + \frac{M_{g_{i+1}}}{2R_i} \right). \quad (\text{A31})$$

Hence we find in the limit  $n_{i+1} - n_i \rightarrow \infty$  for all the shells,

$$\sum_{I=n_i+1}^{n_{i+1}} M_I \longrightarrow m_s(i). \quad (\text{A32})$$

This equation implies that the proper mass of the shell is the sum of the gravitational mass of each object, not the sum of the proper mass of each object.

[1] S. Weinberg, *Gravitation and Cosmology*, (Wiley, New York, 1973).

[2] G.F. Smoot *et al.*, *Astrophys J. Lett.* **396**, L1 (1992).

[3] G.F.R. Ellis, in *Proceedings of 10th International Conference on General Relativity and Gravitation*, edited by B. Bertotti *et al.* (Reidel Dordrech, 1984).



- [4] M. Carfora and K. Piotrkowska, Phys. Rev. **D52**, 4393 (1995);
- [5] T. Futamase, Phys. Rev. Lett. **61**, 2175 (1988); Mon. Not. R. Astron. Soc. **237**, 187 (1989); Prog. Theor. Phys. **86**, 389 (1991); Phys. Rev. **D53**, 681 (1996).
- [6] T. Buchert and J. Ehlers, Astron. Astrophys. **320**, 1 (1997).
- [7] H. Russ, M.H. Soffel, M. Kasai and G. Börner, Phys. Rev. **D56**, 2044 (1997).
- [8] J.P. Boersma, Phys. Rev. **D57**, 798 (1998).
- [9] M. Tanimoto, preprint YITP-98-82 (1998).
- [10] N. Sugiura, K. Nakao and T. Harada, Phys. Rev. **D58**, 103504 (1998).
- [11] S. Bildhauer, Prog. Theor. Phys. **84**, 444 (1990).
- [12] S. Bildhauer and T. Futamase, Mon. Not.R. Astron. Soc. **249**, 126 (1991).
- [13] Y. Sota, T. Kobayashi, K. Maeda, T. Kurokawa, M. Morikawa and A. Nakamichi, Phys. Rev. **D58**, 043502 (1998).
- [14] N. Mustapha, B.A. Bassett, C. Hellaby and G.F.R. Ellis, Class. Quant. Grav. **15**, 2363 (1998).
- [15] D. Ida and K. Nakao, submitted to Prog. Theor. Phys., preprint KUNS-1524 (1999).
- [16] K. Nakao, D. Ida and N. Sugiura, Prog. Theor. Phys. **101**, 47 (1999).
- [17] R.M. Wald, *General Relativity* (University of Chicago Press, Chicago, 1984).
- [18] C.W. Misner, K.S. Thorne, and J.A. Wheeler, *Gravitation* (Freeman, San Francisco, 1973).
- [19] W. Israel, Nuovo Cimento **44B**, 1 (1966); *ibid.* Nuovo Cimento **48B**, 463 (1967); *ibid.* Phys. Rev. **153**, 1388 (1967).
- [20] H. Sato, Prog. Theor. Phys. **76**, 1250 (1986).
- [21] K. Maeda, Gen. Relativ. Gravit. **18**, 931 (1986).
- [22] D. Brill and R.W. Lindquist, Phys. Rev. **131**, 471 (1963).
- [23] N. Sugiura and K. Nakao, in preparation.
- [24] R. Kantowski, Astrophys. J. **155**, 89 (1969)
- [25] C.C. Dyer and R.C. Roeder, Astrophys. J. **189**, 167 (1974)
- [26] P. Schneider, J. Ehlers, and E.E. Falco, *Gravitational Lenses*, Springer-Verlag (New York, 1992)

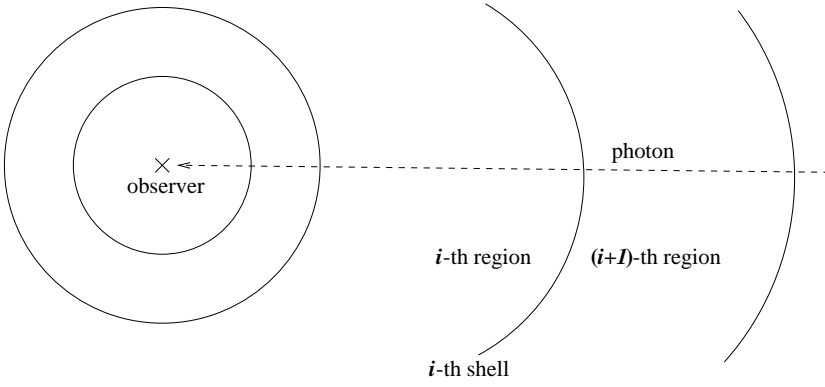


FIG. 1. Dust-shell universe. Between the shells the space is empty.

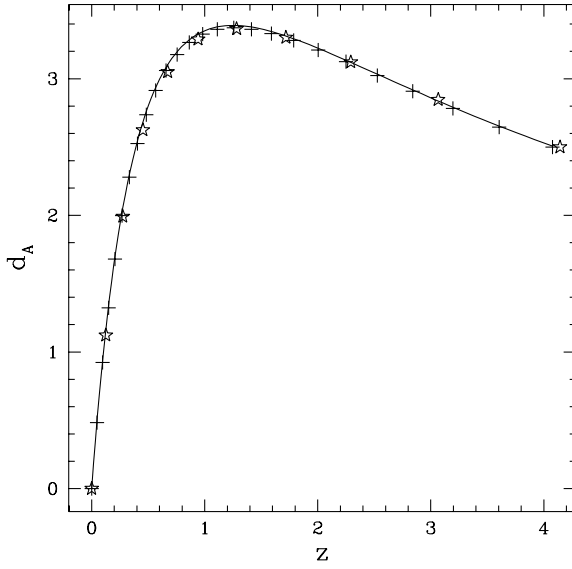


FIG. 2. Angular diameter distance-redshift relation in spatially flat ( $k_c = 0$ ) dust-shell universe for choice A. Data points are shown by cross (+) and star(\*). The number of shells within the initial Hubble horizon  $N_H$  is 4(\*) and 10(+). The total number of shells  $M$  is taken to be  $2.5 \times N_H$ . The solid line shows the  $d_A$ - $z$  relation in a flat FL model with  $H_i = H_{\text{shell}}$ . The redshift of the initial hypersurface is identified with the redshift of the outermost shell for the case  $N_T = 25$ , i.e.,  $z_1 = z(i = 25)$ . As shown in Paper I, the deviation between the flat FL model and the dust-shell universe is almost unrecognizable.

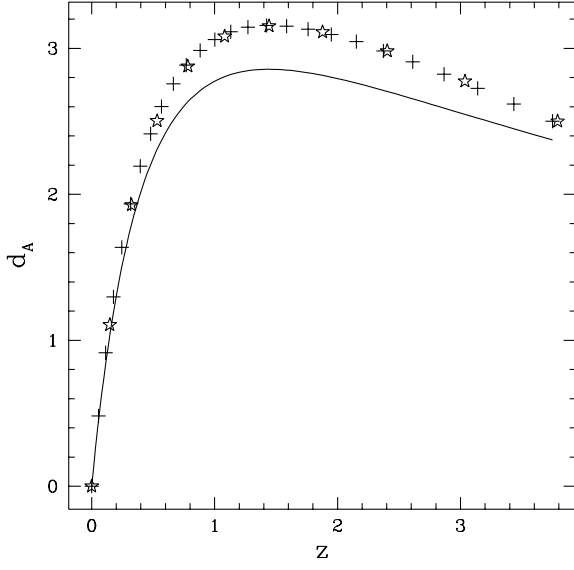


FIG. 3. Same with Fig.1 for open models ( $\Omega = 0.9$ ). The solid line shows the  $d_A$ - $z$  relation in an open FL model with  $\Omega = 0.9, H_I = H_{\text{shell}}, z_I = z(i = 25)$ . We see a large deviation.

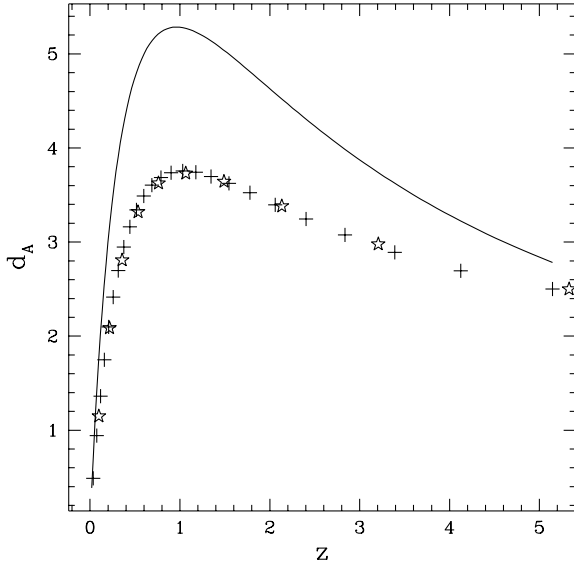


FIG. 4. Same with Fig.1 for closed models ( $\Omega = 1.1$ ). The solid line shows the  $d_A$ - $z$  relation in a closed FL model with  $\Omega = 1.1, H_I = H_{\text{shell}}, z_I = z(i = 25)$ . We see that this FL model does not approximate the dust-shell model.

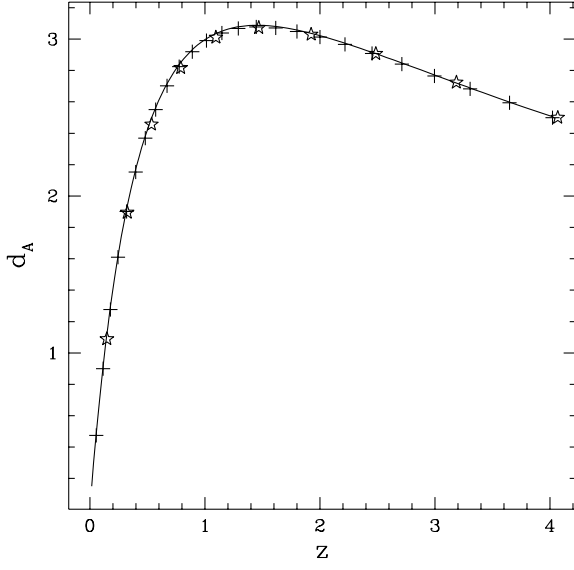


FIG. 5. Angular diameter distance-redshift relation in the open ( $\Omega = 0.9$ ) dust-shell universe for choice B. Compare with Fig.3. The FL relation (solid line) agrees well with the relation of the dust-shell model.

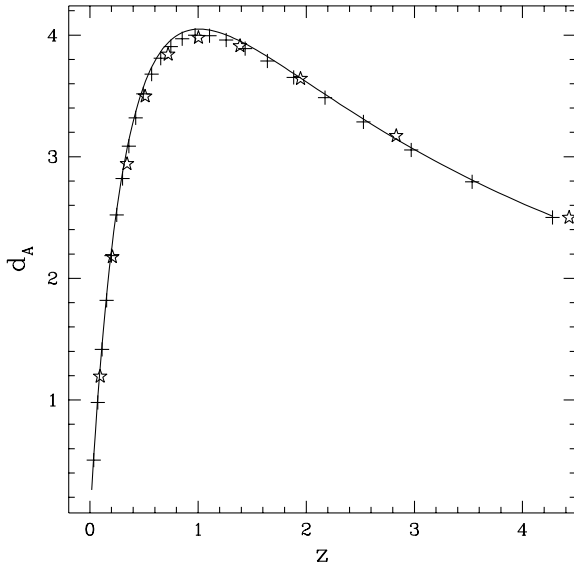


FIG. 6. Angular diameter distance-redshift relation in the closed ( $\Omega = 1.1$ ) dust-shell universe for choice B. Compare with Fig.4. The FL relation (solid line) agrees well with the relation of the dust-shell model.

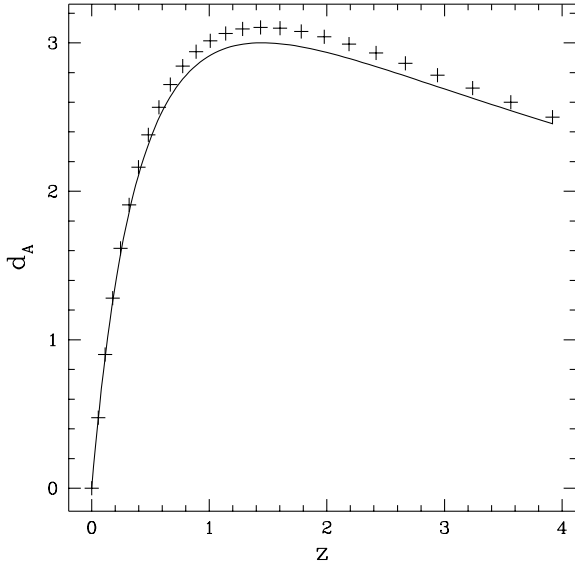


FIG. 7. Angular diameter distance-redshift relation in the dust-shell universe for choice C (open model with  $\Omega = 0.9$ ). We see a mild deviation.